Macromolecules
ARTICLE

Solution Crystallization Behavior of Crystalline−Crystalline Diblock Copolymers of Poly(ethylene oxide)-*block*-poly(ε-caprolactone)

Ryan M. Van Horn,[†] Joseph X. Zheng,[†] Hao-Jan Sun,[†] Ming-Siao Hsiao,[†] Wen-Bin Zhang,[†] Xue-Hui Dong,[†] Junting Xu,[‡] Edwin L. Thomas,[§] Bernard Lotz,[⊥] and Stephen Z. D. Cheng*,[†]

[†]*Maurice Morton Institute and Department of Polymer Science, The University of Akron, Akron, Ohio 44325-3909,* [‡]*Department of Polymer Science and Engineering, Zhejiang University, Hangzhou 310027, China,* [§]*Department of Materials Science and Engineering, Massachusetts Institute of Technology, Cambridge, Massachusetts 02139, and* [⊥]*Institut Charles Sadron, 23, Rue du Loess, Strasbourg 67034, France*

ABSTRACT: The crystallization behavior of crystalline−crystalline (CC) diblock copolymers has been shown to be dependent on the crystallization temperature and relative molecular size of each component. The behavior of copolymers with similar crystallization temperatures is controlled by the block with the larger weight fraction and solvent−polymer interactions. Using samples of poly(ethylene oxide)-*block*-poly-(ε-caprolactone) (PEO-*b*-PCL), dilute solution crystallization methods were investigated to determine their role in crystallization of CC copolymers. A single crystal of one block, either PEO or PCL (the first block), crystallized first with the second block segregated to the crystal basal surfaces. For the first time, solvent quality and homopolymer seeds were introduced to manipulate crystallization of the block with the smaller weight fraction to crystallize first and form the lamellar single crystal. In addition, subsequent crystallization of the tethered chains (the second block) on the surface was also observed, depending upon the molecular weight of the second block and crystallization conditions. These crystallites formed by the second block exhibited preferred orientations on the crystal surface as observed by electron diffraction. It is believed that this orientation was induced by "soft" epitaxy between the fold surfaces of the adjacent single crystals of the first block formed by the initial crystallization.

Introduction

Block copolymers have been the focus of a great volume of research over the past few decades. At the simplest level, the composition of these blocks can vary between amorphous and semicrystalline polymers with a linear architecture. The combinations of amorphous−amorphous (AA), amorphous−crystalline (AC), and crystalline−crystalline (CC) components lead to a wide variety of properties for the resultant diblock copolymers. These properties are also determined by the microstructure of the diblock copolymer, whether phase-separated or a homogeneous melt. Focusing on only those polymers that contain crystalline blocks (AC or CC), a second level of structure on the nanoscale is found for the crystallized block. Factors such as melting temperature of the crystalline block(s) (T_m), glass transition of the amorphous block (T_g), molecular weight, volume fraction, and interaction parameter (χ) play a role in the crystallization of the semicrystalline block copolymers.[1−29]

Of the research in CC diblock copolymers, a large focus has been put on the copolymers with applications in the medical field.[12−30] One prominent system is a diblock copolymer composed of poly(ethylene oxide) (PEO) and poly(ε-caprolactone) (PCL) because of their biocompatibility, biodegradability, and reasonable strength.[15−30] These properties are derived from both their chemical structure as well as their physical structures. Because both PEO and PCL are semicrystalline polymers, their crystallinity greatly affects their mechanical and biorelated properties; therefore, it is important to understand how their crystals grow in this unique architecture.

In most CC diblock copolymer systems, the melting temperature difference between the two blocks is quite large.[12−21] The crystal growth of each block is driven by this difference. During cooling, the block with the higher T_m crystallizes first with the subsequent crystallization of the lower T_m block occurring later. The effects of phase separation and crystallization on the lower T_m block varied. However, the T_m's for PEO and PCL are nearly identical, around 60 °C. This makes their diblock copolymer (PEO-*b*-PCL) crystallization behavior more complicated. Piao and co-workers[28,29] have illustrated that in bulk samples the crystallization order depends largely on the block chain length; i.e., the block with a higher molecular weight will crystallize first, using triblock PCL-*b*-PEO-*b*-PCL. Further studies have shown that this bulk crystallization applies to diblock copolymers as well.[22−27]

In the bulk, the PEO-*b*-PCL crystallization competes with phase separation during cooling from the homogeneous melt state. Crystals form from concentration fluctuations within each of the domains leading to crystallization-induced phase separation. The segregation strength of these copolymers is weak, although their miscibility is up for debate due to variation in experimental results.[12] During solution crystallization, lamellar crystals are formed from dilute solution, usually via the self-seeding technique, with the second block tethered on the basal surfaces.[7,30−34] Here, the segregation, or conformation, of the two blocks in dilute solution is also dependent on the solvent interaction of each block. At high temperatures, the copolymer is dissolved, and the weak segregation determines the local concentration profile of a single chain in dilute conditions. However, similar to the bulk state, once crystallization begins during cooling of the solution, one block will crystallize (nucleate)

*To whom correspondence should be addressed: e-mail scheng@uakron.edu; Tel +1-330-972-6931.

preferentially because of chemical structure parameters, such as molecular weight or solvent quality. Thus, the local concentration of this block will increase following crystallization, and the conformation of the second block will be driven by its solvent interactions as is seen in amorphous−crystalline diblock copolymers. The block that crystallizes first forms the lamellar single crystal. The second crystallizable block may crystallize on the surface of the previously formed lamellar single crystals, as was illustrated by Sun and co-workers,[30] or may stay in its solvated (in solution) or amorphous (dry) state. AFM images showed that the diblock crystals with equal molecular weight for each block exhibited the truncated-lozenge single crystal morphology of the PCL, indicating that PCL had crystallized first. Then, using electron diffraction (ED), they confirmed the appearance of diffraction spots corresponding to the (120) planes of the PEO superimposed with the (110) and (200) diffraction spots of the PCL crystal. Similar results have also been shown for thin film growth of PEO-*b*-poly(L-lactide) (PLLA) copolymers with identical molecular weights between the two blocks.[18−21] Here, the PLLA crystallizes first due to a higher crystallization temperature.

We have found that it is possible under certain conditions to crystallize the block with the shorter chain length first. Two PEO-*b*-PCL samples were used each with one block slightly larger than the other. Using solution crystallization, it was possible to control which block crystallized first through either different solvent conditions or by using homopolymer single crystal seeds. These methods prove that it is possible to induce crystallization of the smaller block prior to the larger block. The block which is closer to the theta-condition in the solvent will crystallize first, or a homopolymer seed can effectively lower the nucleation barrier of the smaller block below the barrier for the larger block. The longer blocks were thus tethered onto the basal surface of the lamellar single crystals. Electron diffraction (ED) experiments show that the secondary block may crystallize on the surface due to either high tethering density or large layer thickness. No diffraction from crystallized surface layers was observed when the shorter block was on the surface. The orientation of the secondary crystallites with respect to the single crystal surface was found to differ from the results found in the literature.[18−21,29]

Experimental Section

Materials. A PEO-*b*-PCL (EOCL-11) sample with number-average molecular weights of 5.0K g/mol (M_n^{PEO}) and 6.3K g/mol (M_n^{PCL}) (w_{PCL} = 0.56) and a PDI of 1.12 was provided by Dr. Xu's lab. A detailed description of the synthetic procedure can be found in the literature.[35] A second sample, EOCL-22, with M_n^{PEO} = 13.5K g/mol for the PEO and M_n^{PCL} = 9.8K g/mol (w_{PCL} = 0.42) and a PDI of 1.09 was synthesized in our group following the procedure for combining ring-opening polymerization with "click" chemistry found in the literature.[36]

The molecular weights were determined by GPC (overall) using polystyrene standards and ^{1}H NMR for the PCL block since it was synthesized from the PEO macroinitiator. A homopolymer PEO sample with M_n^{PEO} = 5K g/mol was also utilized for single crystal seeds. Homopolymer PCL (M_n^{PCL} = 11K g/mol) was purchased from Polymer Source, Inc. *n*-Hexanol was purchased from Acros Organics, and amyl acetate was purchased from Sigma-Aldrich. Both were used as received for dilute solution crystallization.

Equipment and Experiments. Typically, the self-seeding procedure[31] was used to grow uniformly sized polymer single crystals, unless otherwise noted. First, PEO-*b*-PCL and either *n*-hexanol or amyl acetate were mixed at room temperature at dilute solution conditions. The temperature of the mixture was increased to the dissolution temperature (T_d) and kept there for a predetermined amount of time. It was then quenched to room temperature overnight to allow the copolymer to crystallize. The

sample was then placed in an oil bath at the self-seeding temperature for 20 min. At this temperature, about 99% of the crystals dissolved. This leaves only small nuclei to nucleate crystal growth ensuring uniformity. The crystal structure of these nuclei was determined by the primary crystallization of one of the blocks (either PCL or PEO depending on the conditions) to form the central lamellar crystal. The single crystal morphology after isothermal crystallization confirms which block crystallized first in the quenching step. Finally, the sample was quenched to a set isothermal crystallization temperature (T_x) in an oil bath (precision/control ±0.1 °C) until complete crystallization had occurred. Samples were left at T_x for several days to ensure complete crystallization. A similar procedure was used for the growth of homo-PEO single crystals. After the homopolymer single crystals were grown, they were added to a solution of dissolved copolymer at T_x.[32] These homo-PEO crystals acted as the nucleation seeds for subsequent crystallization of the PEO-*b*-PCL on the lateral surface.

Transmission electron microscopy (TEM) and electron diffraction (ED) experiments were conducted to analyze the single-crystal morphology and crystal structure. A Philips TECNAI 12 microscope at an accelerating voltage of 120 kV was used to obtain bright field (BF) and ED images. Samples were prepared by dropping a few aliquots of solution onto a carbon-coated copper grid with a mesh size of 400 μm and allowing the solvent to evaporate. The samples were then stored in a vacuum oven for a few days to ensure complete evaporation.

Atomic force microscopy (AFM) was utilized to determine the crystal thickness for tethering density calculations. A Digital Instruments Nanoscope IIIA AFM was used in the tapping mode to determine the overall thickness of the sandwiched single crystal. The tapping mode with a carefully chosen cantilever tip-to-sample force was best for limiting damage to the single crystal. The typical measurement conditions were a scan size of 20 μm × 20 μm at a scan rate of 1 Hz with operation and resonance frequencies around 300 kHz. The resolution was 512 × 512.

Results and Discussion

Inducing Crystal Growth Based on Changes in Solvent. Single-crystal growth of PCL from dilute solution is typically done in *n*-hexanol,[30,37] while PEO single-crystal growth is done in amyl acetate.[31−34] As such, the EOCL-11 sample was crystallized in *n*-hexanol because the PCL block is larger in weight fraction with its favorable solvent, and EOCL-22 was crystallized in amyl acetate since the PEO block is larger in weight fraction with its favorable solvent. Following the self-seeding procedure for each system, single crystals of the PEO-*b*-PCL samples were grown to verify that the block with a larger M_n formed the lamellar single crystal.

Figures 1 and 2 show the TEM bright field images along with the diffraction patterns for the two single crystals of EOCL-11 (T_x = 26 °C) and EOCL-22 (T_x = 32 °C), respectively. The morphology of the single crystal is the first indication as to which component has formed the central lamellar layer. In Figure 1, the truncated-lozenge morphology of PCL was observed, and thus, the PEO blocks are tethered on both sides of the basal surfaces of the PCL lamellar single crystal. In Figure 2, the square-shaped morphology of PEO single crystals was observed. Hence, the PCL blocks are tethered on both sides of the basal surfaces of the PEO lamellar single crystal. The ED patterns confirm the crystallization of the noted block. The strong (110) and (200) spots of the orthorhombic unit cell of PCL (as labeled in the image) were seen from the truncated-lozenge crystal. This indicates the [001] zone of the crystal was perpendicular to the electron beam, as would be expected for solution-grown single crystals. The four strong (120) spots, representative of the monoclinic PEO unit cell, indicated that the square-shaped
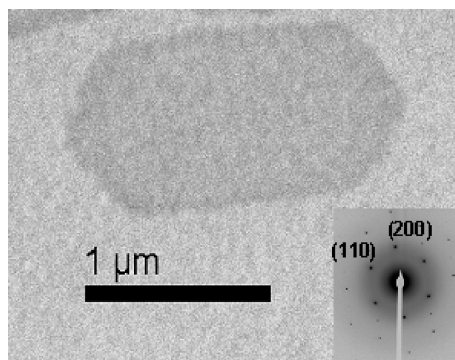
Figure 1. TEM bright field and ED (inset) images of an EOCL-11 single crystal grown in *n*-hexanol at 26 °C with characteristic PCL morphology and diffraction spots.
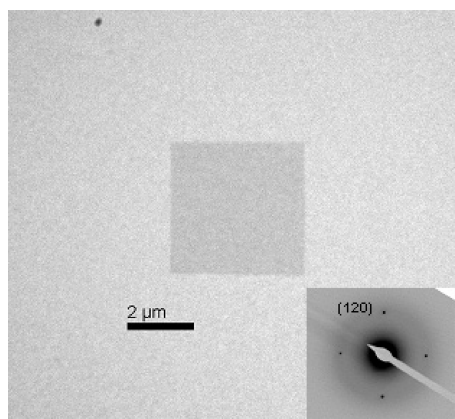

Figure 2. TEM bright field and ED (inset) images of an EOCL-22 single crystal grown in amyl acetate at 32 °C with characteristic PEO morphology and diffraction spots.

single crystal was the [001] zone of PEO. In both cases, it should be noted that diffractions from the tethered block was not observed as in previous studies of PEO-*b*-PCL[30] and PEO-*b*-PLLA.[19] This indicated that the tethered block had not crystallized on the top and bottom surfaces of the single crystal. This may be expected since the tethering density, σ, is assumed to be smaller than the previous studies because the weight fraction of the tethered block was smaller in our case. The relative positions on the surface and the state of the tethered chains are expected to influence their crystallizability.

The PCL crystal thickness, d_{PCL}, of the EOCL-11 sample was 8.0 ± 0.4 nm as determined by AFM ($d_{CRYST} = \nu_{CRYST} \times d_{OVERALL}$).[33,34] The volume fraction of PCL was calculated assuming completely amorphous PEO layers. The tethering density of the PEO blocks on the PCL crystal basal surface was 0.434 nm^{-2}. The R_g of the 5K g/mol PEO was estimated to be 2.6 nm.[38] The resultant reduced tethering density, $\tilde{\sigma}$, where $\tilde{\sigma} = \sigma \pi R_g^2$, was 9.2, which is lower than the onset reduced tethering density of the highly stretched region ($\tilde{\sigma} = 14.3$).[33,34] Therefore, the tethered PEO blocks do not crystallize at room temperature when $\tilde{\sigma} \leq 9.2$.

On the other hand, the PEO crystal thickness, d_{PEO} (calculated assuming amorphous PCL layers), of the EOCL-22 sample was 14.1 ± 0.3 nm, and the tethering density of PCL was 0.212 nm^{-2}. The R_g of the 9.8K g/mol PCL of EOCL-22 was estimated to be 3.3 nm.[38] The $\tilde{\sigma}$ for this system was 7.3 (only about half of the onset reduced tethering density of the highly stretched region). Here, the PCL tethers did not crystallize at room temperature when $\tilde{\sigma} \leq 7.3$. The lack of crystallization may be due to either the low tethering density or a small layer thickness, d_{AM}, of the
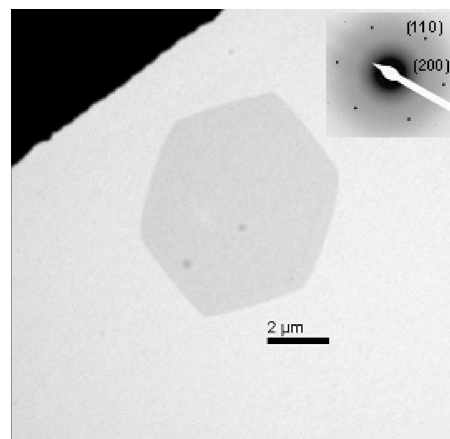

Figure 3. TEM bright field and ED (inset) images of an EOCL-22 single crystal grown in *n*-hexanol at 26 °C with characteristic PCL morphology and diffraction spots with the PCL block as the minority component.

tethers ($d_{AM} = 3.2$ nm for both systems, which is also on the order of R_g). Nucleation may be significantly hindered at room temperature by a lack of material (tethering density) and/or the constraints of a single layer thickness, especially when one end is tethered to the surface.[39–41] It has been shown that at small thicknesses (on the order of R_g) homopolymer crystallization can be hindered because the size (thickness or volume) does not support a stable nucleus; however, some reports show a stable crystal with a *d*-value larger than the film thickness. In our case, the tethering of one end hinders the mobility of the chains to form these crystals even if a stable nucleus could be formed. In the previous studies of CC copolymers, assuming that the PEO was in the theta-state, the $\tilde{\sigma}$ was estimated from the data in the literature to be 23.5 for PEO-*b*-PCL[30] and 13.2 for the PEO-*b*-PLLA.[14] One should also be aware that the highly dislocated nature of the single crystals may release the constraints of the single tethered layer, contrary to the current study, allowing the crystallization to occur more easily.[7,40] In addition, thin film samples have readily available amorphous copolymer in the vicinity to supply material and facilitate crystallization. We are currently investigating these factors and their role in the tether crystallization.

To determine the effects of solvent type on the crystallization of the two PEO-*b*-PCL copolymers, the solvent type used for each was exchanged; thus, amyl acetate was used for EOCL-11 and *n*-hexanol was used for EOCL-22. Figure 3 shows the single crystal grown from EOCL-22 in *n*-hexanol. These crystals were grown by directly quenching the solution from T_d to $T_x = 26$ °C. The morphology of the single crystal is an indication that the PCL block, which is shorter for EOCL-22 ($w_{PCL} = 0.42$), was crystallized first. This result differed from crystallization in amyl acetate where the PEO block crystallized (see Figure 2). For this system, the solvent interaction overrides the propensity for the larger block to crystallize first. The *n*-hexanol is a slightly poorer solvent for PCL; therefore, the PCL block forms the lamellar single crystal with PEO tethered on the surface. The ED pattern shown in the inset of Figure 3 supports the conclusion that the PCL forms the sandwiched single crystal. Again, no crystallization of the PEO component on the surface was observed after quenching to room temperature. The tethering density of the PEO blocks was 0.274 nm^{-2}, and $\tilde{\sigma} = 15.2$ ($R_g = 4.2$ nm). Thus, the PEO tethers still do not crystallize at room temperature when $\tilde{\sigma} \leq 15.2$. This is a little unexpected since the PEO tethers were above the 14.3 transition
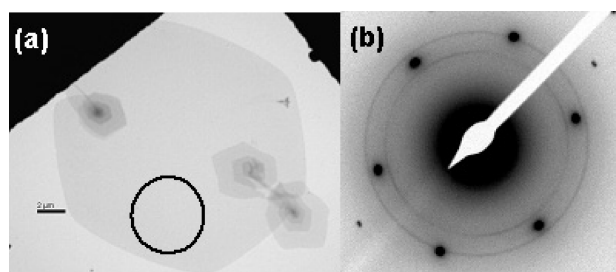
Figure 4. TEM bright field (a) and ED (b) images of an EOCL-22 with screw dislocations. The diffraction image indicates that PEO crystallization was induced by the double layer of PEO tethers under the dislocation.

value; however, the value is close considering the estimation of R_g.

There was some evidence, on the other hand, that $\tilde{\sigma} = 15.2$ may be near the transition for crystallization. In a small population of the crystals, screw dislocations could be found near the intersection of two [110] growth fronts (Figure 4a). ED experiments were performed on the single-layer area (indicated by the circle in Figure 4a) of this crystal and are shown in Figure 4b. From this ED pattern, isotropic diffraction rings with d-spacings of 0.463 and 0.39 nm were observed. The inner ring (d-spacing = 0.463 nm) is indexed as the (120) diffraction of PEO, while the outside ring (d-spacing = 0.390 nm) consists of overlapped (hkl) diffractions. They are the overlapped diffractions by combining the ($\bar{1}$32), (032), (112), ($\bar{2}$12), ($\bar{1}$24), ($\bar{2}$04), and (004) diffractions.[5,7] The tether crystallization of these crystals containing dislocations was probably caused by the double layer of PEO tethers underneath the crystallized PCL dislocation. The double layer effectively increases the tethering density, likely 2-fold, providing a nucleation site. Once nucleation occurs in this double layer, crystal growth propagates throughout the single crystal, even in the single-layer region. This propagation indicates that when $\tilde{\sigma} = 15.2$, crystallization may occur, but nucleation in the single layer of PEO is suppressed at room temperature. Further investigation is currently underway.

EOCL-11 in amyl acetate does not crystallize into dendritic or single crystals. The interaction of PCL with amyl acetate dominates the assembly in solution and prevents crystallization of the PEO block. This may also have been caused by the lower molecular weights as compared to EOCL-22. However, the proof of principle is still shown by the EOCL-22 block where w_{PCL} is lower than 0.50. The ability to crystallize the smaller block is further enhanced by utilizing homopolymer seeds to create an epitaxial environment to induce crystallization.

Inducing Crystal Growth through Homopolymer Crystal Seeds. Single crystals of the homo-PEO sample with $M_n^{PEO} = 5K$ g/mol were used as seeds in *n*-hexanol at 26 °C to epitaxially grow single crystals of EOCL-11. First, the homo-PEO was crystallized into single crystals with uniform shape and size by the self-seeding procedure.[32] An EOCL-11/*n*-hexanol solution at the same concentration was dissolved and placed into the same isothermal temperature bath. After 10 min, a small aliquot of the homo-PEO solution (containing homo-PEO crystal seeds) was added to the block copolymer solution. The sample was allowed to crystallize for another 2 days before analysis.

The square-shaped habit of the crystal seen in the center of Figure 5 indicates that the PEO block of EOCL-11 has crystallized starting at the periphery of the homo-PEO seed. The darker section is indicative of a thicker layer of the EOCL-11 single crystal grown on the lateral surface of the
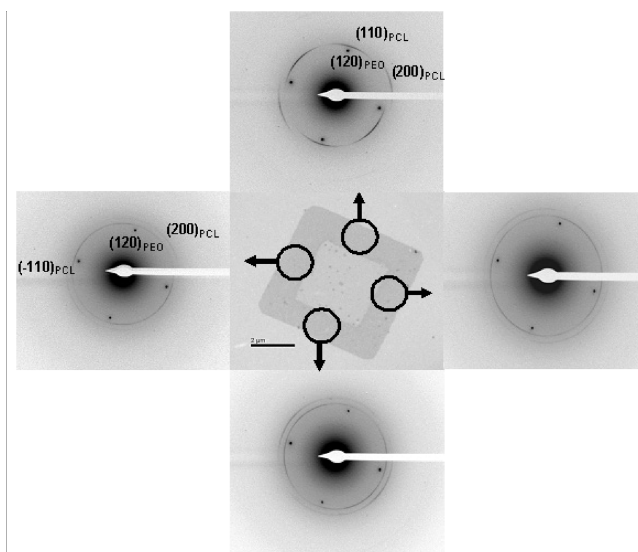

Figure 5. TEM bright field image of the homo-PEO single crystal (center) seeded crystallization of EOCL-11 (outer layer) (middle). The darker section indicates the thicker, diblock component. ED patterns of the EOCL-11 crystal for each sector are placed around the central bright field image.

homo-PEO crystal. The lighter, central section is the homo-PEO single crystal. The PCL block is now the tethered layer on both fold surfaces of the PEO single crystal. The PEO blocks crystallized first because the homo-PEO seed decreased the nucleation barrier for PEO crystal growth, indicating that the decrease of the PEO nucleation barrier was stronger than both the enthalpic contribution from PCL crystallization and the entropic contribution of tethered chain crowding on the PEO surface. Electron diffraction was used to analyze the existence of a central layer PEO crystal (block sandwiched structure) as well as determine any crystallization in the PCL layers.

The images surrounding the TEM bright field image in Figure 5 are the ED patterns collected from the subsequent sectors of the PEO single crystal. In these ED patterns, the four (120) diffraction spots of the PEO monoclinic unit cell were observed, indicating that both the thicker (attributed to copolymer) and thinner (attributed to homo-PEO) sections belong to one single crystal. This is also further evidence that the PEO block crystallized on the lateral surface of the homo-PEO single crystal to form the middle of the sandwich structure. Moreover, the PEO stems in the crystal are oriented parallel to the lamellar normal. In Figure 5, additional diffraction arcs were observed as well. At first glance, they may appear as rings; however, closer inspection reveals that the intensity of the diffraction increases in specific arcs around the circumference. These diffraction arcs are representative of PCL crystallization in the two tethered layers.

The best example is the ED pattern at the top of Figure 5. The four arcs immediately outside the (120) spots of the PEO are at a d-spacing of 0.418 nm, which are attributed to the d-spacing for the (110) planes in the orthorhombic PCL crystals. The two outer arcs are at a d-spacing of 0.375 nm, which corresponds to the d-spacing for the (200) planes. The appearance of these pairs of diffraction arcs indicates that the PCL blocks have crystallized to form small crystallites, as was seen by Sun et al.[30] However, these PCL crystals possess only some orientation on the PEO single crystal basal surfaces, not perfect orientation, which would be supported by diffraction spots.

The thickness of the PEO single crystal was calculated as 16.0 nm assuming a crystalline density for the PCL chains. The difference in ν_{PEO} calculated from either the amorphous or crystalline PCL density is only 0.01. It was assumed that the PCL is not 100% crystalline; however, this assumption was not significant in calculating the PEO thickness. The tethering density of the PCL on the PEO single crystal surface is calculated to be 1.19 nm^{-2}, which is quite high for tethered polymer chains. Although the PCL chains are small, with an estimated R_g of 2.6 nm,[39] the $\tilde{\sigma}$ value is 25.4. This value greatly exceeds the onset of entering the highly stretched region of 14.3.[34] This dense packing of chains facilitates their ability to crystallize. Therefore, we can at least conclude that the necessary condition for the tethered chains to crystallize requires a reduced tethering density greater than the onset of entering the highly stretched region. Also, it is not quantitatively clear what affect PCL crystallization has on the free energy for determining the equilibrium PEO thickness and whether this affects the measured tethering density. Further experiments are currently underway to elaborate on this.

Tethered Chain Crystallization. In Figure 4b, PEO crystallization was observed on the single crystal surface due to nucleation in the double-layer region below the screw dislocation in the form of two isotropic rings. These rings provide information on the orientation of the PEO crystallites on the PCL crystal surface. The appearance of rings indicates that the PEO crystallites did not have a preferential lateral orientation on the surface, unlike the PCL tethered crystallization case (Figure 5). The propagation of PEO crystallization was likely to occur from multiple nucleation events in the double layer below each of the screw dislocations. These nucleation events may have different orientations resulting in an isotropic alignment of crystallites on the surface. The (120) and the overlapped ($\bar{1}$32), (032), (112), ($\bar{2}$12), ($\bar{1}$24), ($\bar{2}$04), and (004) diffraction rings are evidence that the c-axis, or stem direction, of the PEO crystallites is not parallel with the electron beam (surface normal).[5,7] However, it is difficult to determine the tilting angle or perpendicular orientation from ring patterns. The origin of this unique stem orientation may be related to recent work in confined crystallization of PEO by Hsiao and co-workers.[7,42]

In Figure 5, the stem orientation, or the c-axis, of the PCL crystallites is parallel to the electron beam, as well as the PEO surface normal, since the observed diffractions are associated with the [001] zone of the PCL crystallites, (110) and (200) arcs. The lateral orientation of the PCL tethered crystals was also analyzed from the ED patterns in Figure 5. The arcs indicate that the PCL crystallites have some lateral orientational order on the PEO crystal surface. Because they exhibit diffraction arcs or rings and not diffraction spots, they were not single crystalline as was seen in previous studies. Again, it should be noted that although some ED patterns appear to exhibit rings instead of arcs, the varying intensity around the circumference is evidence of some orientation on the surface. One explanation is that several nucleation events have occurred in the PCL layer during cooling, unlike the previous results where a single-crystal diffraction pattern implies the occurrence of a single nucleation event. The other is that there was no "hard" epitaxy to influence all crystallites (in the event of several nucleation events) to align all crystals perfectly with the same orientation, providing a single crystal pattern in the absence of a singular crystal being formed. From Figure 5, it was observed that there was a general crystallite orientation on the crystal surface itself. The (110) diffraction arcs of the PCL are nearly aligned with the (120) diffraction spots of the PEO.
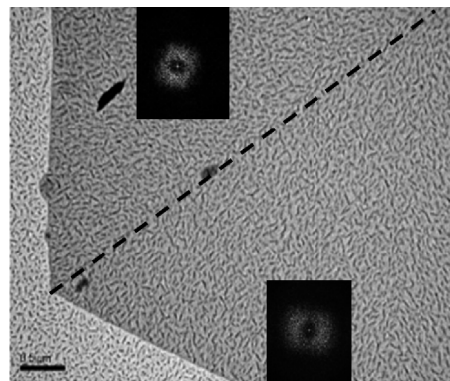

Figure 6. PE decoration of homo-PCL single crystal with fast Fourier transforms (FFT) of the two sectors. Alignment of the PE crystallites indicates that the fold direction is perpendicular to the [110] growth direction. Scale bar: 0.5 μm.

This proves that the [110] direction of the PCL crystallites is parallel to the [120] direction of the PEO single crystal, though not exclusively for all crystallites because of the observed arcs. In other words, although the c-axis is oriented parallel to the electron beam, the ab-plane is only partially oriented in the plane perpendicular to the beam. As seen in the bottom ED pattern, this observation cannot be concluded to be absolutely true but does occur frequently.

The origin of such orientation is most likely due to "soft" epitaxy between the fold surfaces of the two types of crystals. Figure 6 shows a polyethylene-decorated (PE) homo-PCL crystal, specifically two adjacent (110) growth faces. In PE decoration, an oligomeric polyethylene is evaporated under vacuum and allowed to deposit on the surface of the crystal. Once the system returns to ambient conditions, the PE forms small crystallites that have a preferred orientation due to epitaxial alignment with the fold surface. From the bright field image as well as the fast Fourier transform (FFT) patterns, the preferential orientation of the PE crystallites is approximately perpendicular to the (110) growth face. This is an indication that the fold direction in PCL crystals is perpendicular to the [110] growth direction.[43-45] It has been shown previously that the fold direction of PEO is perpendicular to the [120] growth direction. Therefore, soft-epitaxy cooperation between these two fold surfaces should cause the orientation of the (110) diffraction of the PCL crystallites with the (120) diffraction of the PEO single crystal. It was also observed that the orientation of the PCL varies slightly between sectors. For the topmost sector of Figure 5, the diffraction pattern shows that the (110) arc of the PCL crystallites is parallel to the growth surface. A similar result is seen in the right-hand sector and diffraction pattern. However, in the left-hand sector, the ($\bar{1}$10) spot is aligned with the growth face. This is not unexpected since the fold direction of the PCL unit cell is along the set of (110) planes depending on the growth face (this is illustrated by the PEO single crystal discussed here). Figure 7 is a schematic of the "soft" epitaxy between the various fold surfaces. The unit cell for PCL and PEO are shown at the top (looking parallel to the c-direction). The bottom of Figure 7 illustrates the parallel alignment of either (110)$_{PCL}$ (left) or ($\bar{1}$10)$_{PCL}$ (right) with the (120)$_{PEO}$ growth face. In fact, the d-spacings of the (120)$_{PEO}$ and (110)$_{PCL}$ (and, by definition, ($\bar{1}$10)$_{PCL}$) are 0.463 and 0.418 nm, respectively. This near match of the space between the folds (not taking into account fold volume) also supports a "soft" epitaxy between the two types of crystals.

It is equally interesting that the orientation of these PCL small crystals was located on both sides of the PEO single
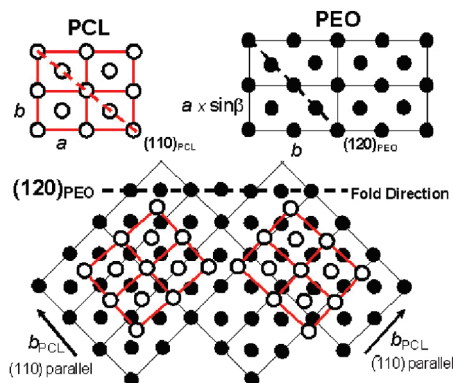
Figure 7. Schematic of "soft" epitaxy between PCL crystallites and the PEO single crystal surface: the unit cells of PCL and PEO (top); alignment of $(110)_{PCL}$ and $(120)_{PEO}$ (bottom left); and alignment of the $(110)_{PCL}$ and $(120)_{PEO}$ (bottom right). These two different alignments were observed in the ED patterns of Figure 5.

crystal since little deviation from this orientation was observed in the ED pattern. Because of the sandwiched structure, the PCL small crystals on both sides cannot communicate with each other, resulting in coupled orientation. Therefore, this orientation must be associated with some type of "soft" epitaxy on the folded surfaces of the PEO block single crystals. Considering that the angle between the (110) growth planes of the PCL is 50° and the angle between the (120) growth planes of PEO is 90°, the "soft" epitaxy of the two fold surfaces would not always result in perfect alignment because of this mismatch. In addition, only one diffraction spot was oriented epitaxially with the PEO (120) spot because of the difference in angles between the dominant growth sectors of the two blocks. This indicates that the epitaxial relationship may be established during nucleation or the early stages of crystal growth. The lack of this orientation in the PEO tether crystallization is most probably due to the difference in *c*-axis (stem) orientation in the crystallites. The role of tethering density, layer thickness, and supercooling for the crystallization of the tethered layer is currently under investigation and will be discussed in a future publication.

Conclusion

It has been shown that it is possible to use different solvent conditions or homopolymer seeds to induce crystallization of the smaller block in PEO-*b*-PCL copolymers where the crystallization temperatures are similar and the crystallization behavior is determined by the weight fraction of each block. With varying solvent conditions, the block that is closer to the theta-condition crystallizes first because in good solvent it will not crystallize and in poor solvent precipitation occurs. Thus, it is possible to control the morphology of the single crystals using different solvents. The homo-PEO crystal acts as a seed to lower the nucleation barrier associated with crystallizing the PEO in the EOCL-11 sample. The PCL block was tethered to the fold surface of the PEO sandwiched crystal and crystallized after the PEO lamella was formed. The PCL crystallites have a *c*-axis orientation that is parallel to the surface normal and some orientation of the *ab*-plane along the surface. This results in the appearance of diffraction arcs instead of diffraction spots associated with the (110) and (200) planes of the PCL. The (110) planes of the PCL crystallites align parallel to the (120) planes of the PEO crystals possibly due to soft epitaxy of the two fold surfaces.

References and Notes

(1) Hamley, I. W. *Adv. Polym. Sci.* **1999**, *148*, 113.
(2) Loo, Y. L.; Register, R. A. Crystallization within block copolymer mesophases. In *Developments in Block Copolymer Science and Technology*; Hamley, I. W., Ed.; Wiley: New York, 2004.
(3) Müller, A. J.; Balsamo, V.; Arnal, M. L. *Adv. Polym. Sci.* **2005**, *190*, 1.
(4) Huang, P.; Zhu, L.; Guo, Y.; Ge, Q.; Jing, A. J.; Chen, W. Y.; Quirk, R. P.; Cheng, S. Z. D.; Thomas, E. L.; Lotz, B.; Hsiao, B. S.; Avila-Orta, C. A.; Sics, I. *Macromolecules* **2004**, *37*, 3689.
(5) Zhu, L.; Cheng, S. Z. D.; Calhoun, B. H.; Ge, Q.; Quirk, R. P.; Thomas, E. L.; Hsiao, B. S.; Yeh, F.; Lotz, B. *J. Am. Chem. Soc.* **2000**, *122*, 5957.
(6) Takeshita, H.; Ishii, N.; Araki, C.; Miya, M.; Takenaka, K.; Shiomi, T. J. *J. Polym. Sci., Polym. Phys. Ed.* **2004**, *42*, 4199.
(7) Hsiao, M.-S.; Zheng, J. X.; Leng, S.; Van Horn, R. M.; Quirk, R. P.; Thomas, E. L.; Chen, H.-L.; Hsiao, B. S.; Rong, L.; Lotz, B.; Cheng, S. Z. D. *Macromolecules* **2008**, *41*, 8114.
(8) Weimann, P. A.; Hajduk, D. A.; Chu, C.; Chaffin, K. A.; Brodil, J. C.; Bates, F. S. *J. Polym. Sci., Polym. Phys. Ed.* **1999**, *37*, 2053.
(9) Wang, L.; Xu, J.-T.; Ding, P.-J.; Fan, Z.-Q. *Chin. J. Polym. Sci.* **2006**, *24*, 473.
(10) Castillo, R. V.; Müller, A. J.; Lin, M.-C.; Chen, H.-L.; Jeng, U.-S.; Hillmyer, M. A. *Macromolecules* **2008**, *41*, 6154.
(11) Sun, L.; Liu, Y.; Zhu, L.; Hsiao, B. S.; Avila-Orta, C. A. *Polymer* **2004**, *45*, 8181.
(12) Castillo, R. V.; Müller, A. J. *Prog. Polym. Sci.* **2009**, *34*, 516.
(13) Jeong, S. I.; Kim, B. S.; Lee, Y. M.; Ihn, K. J.; Kim, S. H.; Kim, Y. H. *Biomacromolecules* **2004**, *5*, 1303.
(14) Albuerne, J.; Márquez, L.; Müller, J.; Raquez, J. M.; Degée, P.; Dubóis, P.; Castelletto, V.; Hamley, I. W. *Macromolecules* **2003**, *36*, 1633.
(15) Fujiwara, T.; Kimura, Y. *Macromol. Biosci.* **2002**, *2*, 11.
(16) Shin, D.; Shin, K.; Aamer, K. A.; Tew, G. N.; Russell, T. P. *Macromolecules* **2005**, *38*, 104.
(17) Yang, J.; Zhao, T.; Cui, J.; Liu, L.; Zhou, Y.; Li, G.; Zhou, E.; Chen, X. *J. Polym. Sci., Polym. Phys. Ed.* **2006**, *44*, 3215.
(18) Sun, J.; Hong, Z.; Yang, L.; Tang, Z.; Chen, X.; Jing, X. *Polymer* **2004**, *45*, 5969.
(19) Yang, J.; Zhao, T.; Zhou, Y.; Liu, L.; Li, G.; Zhou, E.; Chen, X. *Macromolecules* **2007**, *40*, 2791.
(20) Huang, S.; Jiang, S.; An, L.; Chen, X. *J. Polym. Sci., Polym. Phys. Ed.* **2008**, *46*, 1400.
(21) Huang, S.; Jiang, S.; Chen, X.; An, L. *Langmuir* **2009**, *25*, 13125.
(22) He, C.; Sun, J.; Zhao, T.; Chen, X.; Jing, X. *Biomacromolecules* **2006**, *7*, 252.
(23) He, C.; Sun, J.; Deng, C.; Zhao, T.; Deng, M.; Chen, X.; Jing, X. *Biomacromolecules* **2004**, *5*, 2042.
(24) Xu, Y.; Zhang, Y.; Fan, Z.; Li, S. *J. Polym. Sci., Polym. Phys. Ed.* **2010**, *48*, 286.
(25) Bogdanov, B.; Vidts, A.; Schacht, E.; Berghmans, H. *Macromolecules* **1999**, *32*, 726.
(26) Takeshita, H.; Katsuhiko, F.; Ohnishi, T.; Ohkubo, T.; Miya, M.; Takenaka, K.; Shiomi, T. *Polymer* **2006**, *47*, 8210.
(27) Gan, Z. H.; Jiang, B. Z.; Zhang, J. *J. Appl. Polym. Sci.* **1996**, *59*, 961.
(28) Piao, L.; Dai, Z.; Deng, M.; Chen, X.; Jing, X. *Polymer* **2003**, *44*, 2025.
(29) Piao, L.; Deng, M.; Chen, X.; Jiang, L.; Jing, X. *Polymer* **2003**, *44*, 2331. Arnal, M. L.; Lopez-Carrasquero, F.; Laredo, E.; Müller, A. J. *Eur. Polym. J.* **2004**, *40*, 1461.
(30) Sun, J.; Chen, X.; He, C.; Jing, X. *Macromolecules* **2006**, *39*, 3717.
(31) Lotz, B.; Kovacs, A. J. *Kolloid Z. Z. Polym.* **1966**, *209*, 97.
(32) Chen, W. Y.; Li, C. Y.; Zheng, J. X.; Huang, P.; Zhu, L.; Ge, Q.; Quirk, R. P.; Lotz, B.; Deng, L.; Wu, C.; Thomas, E. L.; Cheng, S. Z. D. *Macromolecules* **2004**, *37*, 5292.
(33) Chen, W. Y.; Zheng, J. X.; Cheng, S. Z. D.; Li, C. Y.; Huang, P.; Zhu, L.; Xiong, H.; Ge, Q.; Guo, Y.; Quirk, R. P.; Lotz, B.; Deng, L.; Wu, C.; Thomas, E. L. *Phys. Rev. Lett.* **2004**, *93*, 028301.
(34) Zheng, J. X.; Xiong, H.; Chen, W. Y.; Lee, K.; Van Horn, R. M.; Quirk, R. P.; Lotz, B.; Thomas, E. L.; Shi, A.-C.; Cheng, S. Z. D. *Macromolecules* **2006**, *39*, 641.
(35) Du, Z.-X.; Yang, Y.; Xu, J.-T.; Fan, J.-T. *J. Appl. Polym. Sci.* **2007**, *104*, 2986.

(36) Yang, L.-P.; Dong, X.-H.; Pan, C.-Y. *J. Polym. Sci., Part A: Polym. Chem.* **2008**, *46*, 7757.

(37) Iwata, T.; Doi, Y. *Poly. Int.* **2002**, *51*, 852.

(38) The R_g's for PEO and PCL were estimated for chains in the theta-condition for both solvents using $R_g^2 = b^2 N_b/6$ from: Rubenstein, M.; Colby, R. H. *Polymer Physics*; Oxford University Press: New York, 2004, where $b^{PEO} = 0.8$ nm and $b^{PCL} = 0.7$ nm. The theta-solvent assumption is validated by the ability to crystallize each block in the solvents within the temperature range studied and preliminary results from LLS in Prof. Chi Wu's group at the Chinese University of Hong Kong that indicate R_h measurements of both PCL and PEO in n-hexanol were difficult to obtain.

(39) Van Horn, R. M.; Cheng, S. Z. D. Crystallization in polymer thin films: Morphology and growth. In *Polymer Thin Films*; Tsui, O. K. C., Russell, T. P., Eds.; World Scientific: River Edge, NJ, 2008.

(40) Zhu, L.; Cheng, S. Z. D.; Calhoun, B. H.; Ge, Q.; Quirk, R. P.; Thomas, E. L.; Hsiao, B. S.; Yeh, F.; Lotz, B. *Polymer* **2001**, *42*, 5829.

(41) Massa, M. V.; Dalnoki-Veress, K. *Phys. Rev. Lett.* **2004**, *92*, 255509.

(42) Hsiao, M.-S.; Zheng, J. X.; Van Horn, R. M.; Quirk, R. P.; Thomas, E. L.; Chen, H.-L.; Lotz, B.; Cheng, S. Z. D. *Macromolecules* **2009**, *42*, 8343.

(43) Chen, J.; Cheng, S. Z. D.; Wu, S. S.; Lotz, B.; Wittmann, J.-C. *J. Polym. Sci., Polym. Phys. Ed.* **1995**, *33*, 1851.

(44) Wittmann, J.-C.; Lotz, B. *Makromol. Chem., Rapid Commun.* **1982**, *3*, 733.

(45) Wittmann, J.-C.; Lotz, B. *J. Polym. Sci., Polym. Phys. Ed.* **1985**, *23*, 205.